Coherent photoproduction of light vector mesons off nuclear targets in the dipole picture

Haimon Otto Melchiors Trebien
In collaboration with: Cheryl Henkels, Emmanuel G. de Oliveira and Roman Pasechnik

Florianópolis, 2025

Universidade Federal de Santa Catarina, Universidade do Estado de Santa Catarina

Presentation

1. Dipole Formalism
2. Exclusive Production of Vector Mesons from the Proton
3. Photoproduction of Vector Mesons in ultraperipheral nuclear collisions
4. Conclusion
5. Future Perspectives

Final States

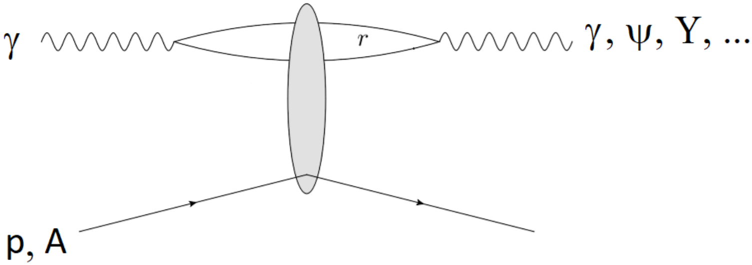

Within the dipole model, only final states with $J^{PC} = 1^{--}$ are selected.

- Exclusive production of the mesons ρ, ω, and ϕ, as well as their excited states.
- Extension to the nuclear case via the Glauber-Gribov theory.

Photon Interaction with the Target Proton

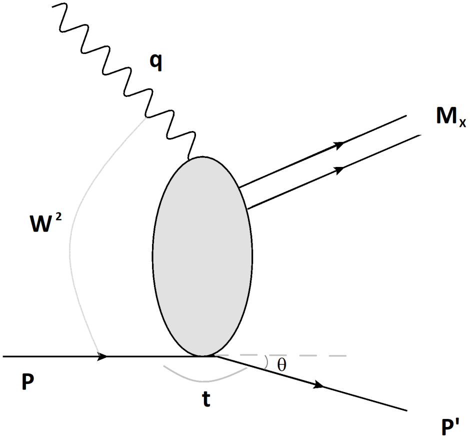

Variáveis cinemáticas:

$$W^2 = (P+q)^2\,, \quad Q^2 = -q^2\,.$$

$$t = (P' - P)^2\,, \quad x = \frac{M_X^2 + Q^2}{W^2 + Q^2}\,.$$

Para altas energias:

$$t \simeq -|\vec{\Delta}_T|^2\,.$$

Diagram and the Dipole Model

Total amplitude is the product of subprocesses.

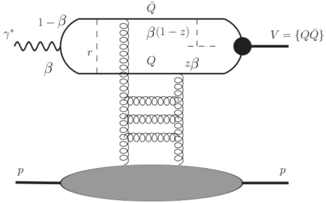

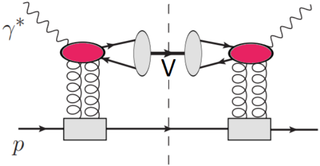

Wave Function $\Psi_{\gamma_{T,L}}^{(\mu,\bar{\mu})}$

The perturbative calculation in light-cone variables is well-known in the literature.
The wave function $\Psi_{\gamma_{T,L}}^{(\mu,\bar{\mu})}$ is given by perturbative calculations, with definitions for the operators acting in transverse (T) and longitudinal (L) polarization.

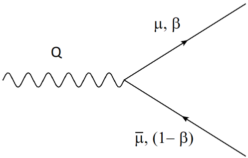

Dipole-Proton Cross Section – GBW Model

The phenomenological model proposed by Golec-Biernat and Wusthoff is one of the simplest for describing the color dipole cross section:

- For small dipoles ($r \ll 1/Q_S$): color transparency
- For large dipoles ($r \gg 1/Q_s$): cross section saturates to a constant value σ_0

The most recent fit considers low momentum scales.

Dipole-Proton Cross Section - bCGC Model

The bCGC model interpolates between the Balitsky-Fadin-Kuraev-Lipatov (BFKL) equation and the Balitsky-Kovchegov (BK) equation. The model is divided into two distinct regions:

$$N(x, \mathrm{r}, \mathrm{b}) = \begin{cases} N_0 \left(\frac{r\,Q_s}{2}\right)^{2\left[\gamma_s + \left(\frac{1}{\eta \Lambda Y}\right) \ln\left(\frac{2}{rQ_s}\right)\right]}, & rQ_s \leq 2 \\ 1 - e^{-A \ln^2(B\,r\,Q_s)}, & rQ_s > 2 \end{cases}, \qquad (1)$$

where $Y = \ln(1/x)$, and

$$Q_s \equiv Q_s(x, b) = \left(\frac{x_0}{x}\right)^{\Lambda/2} \left[\exp\left(-\frac{b^2}{2B_{\mathrm{CGC}}}\right)\right]^{1/(2\gamma_s)}, \qquad (2)$$

is the saturation scale dependent on the impact parameter.

Dipole-Proton Cross Section - bSat Model

With the aim of describing HERA data, the parametrization was initially proposed by Kowalski and Teaney and has an exponential form:

$$N(x, \mathrm{r}, \mathrm{b}) = 1 - \exp\left(-\frac{\pi^2}{2N_c} r^2 \alpha_S(\mu^2) xg(x, \mu^2) T(b)\right) , \qquad (3)$$

where $xg(x, \mu^2)$ represents the gluon density of the target proton.

The adopted gluon distribution is the CT14LO PDF, and

$$T(b) = \frac{1}{2\pi B_G} e^{-b^2/2B_G} \qquad (4)$$

with $B_G = 4.25$ GeV^2.

Dipole-Proton Cross Section

Two considerations are essential:

- Color transparency: for when $r \to 0$.
- Saturation: when $r \gg 0$.

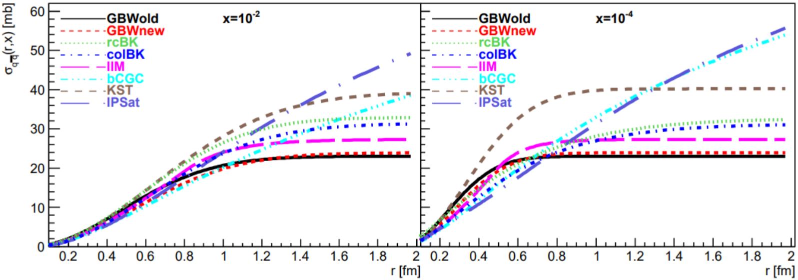

AdS/QCD correspondence

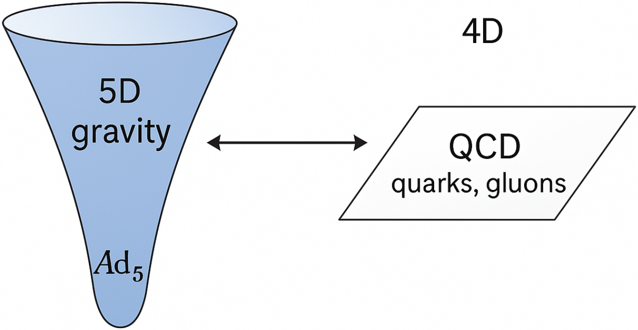

Holographic Meson Wavefunction

The semi-classical AdS/QCD approximation is given by

$$\phi(\beta, \zeta, \varphi) = \frac{\Phi(\zeta)}{\sqrt{2\pi\zeta}} f(\beta) e^{iL\varphi} \tag{5}$$

where $\zeta = \sqrt{\beta(1-\beta)}r$. The function $\Phi(\zeta)$ satisfies the Schrödinger equation

$$\left(-\frac{d^2}{d\zeta^2} - \frac{1-4L^2}{4\zeta^2} + U(\zeta)\right)\Phi(\zeta) = M^2\Phi(\zeta) \tag{6}$$

in which $U(\zeta)$ is an effective confinement potential. The dependence on β is known in the literature and given by $f(\beta) \sim \sqrt{\beta(1-\beta)}$.

Soft-wall Model and Analytical Solution

The soft-wall model is given by:

$$U(\zeta) = \kappa^4\zeta^2 + 2\kappa^2(J-1)\,. \tag{7}$$

We obtain as eigenvalues of the Schrödinger equation:

$$M^2 = 4\kappa^2\left(n + \frac{J}{2} + \frac{L}{2}\right)\,. \tag{8}$$

Solving the Schrödinger equation, we obtain the dynamical part of the AdS/QCD wavefunction, which has the analytical solution:

$$\Phi_{n,L}(\beta,\zeta) = \kappa^{1+L}\sqrt{\frac{2n!}{(n+L)!}}\zeta^{1/2+L}\exp\left(\frac{-\kappa^2\zeta^2}{2}\right)L_n^L(\kappa^2\zeta^2)\,, \tag{9}$$

where $L_n^L(\kappa^2\zeta^2)$ are Laguerre polynomials.

The κ Parameter of the Effective Confinement Potential

For each meson family, we have: $\kappa = M_{n=0}/\sqrt{2}$

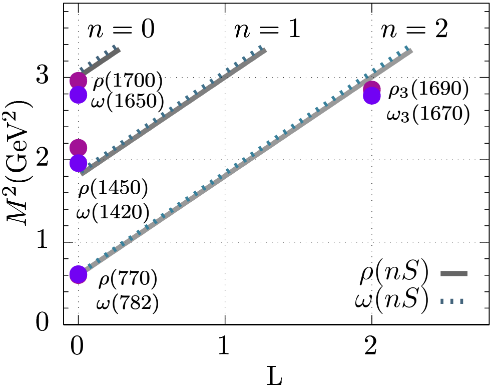

Spectroscopy of the ρ and ω mesons, as well as their excited states. A κ that varies with the meson family can provide a good description of the excited states.

Meson Wavefunction

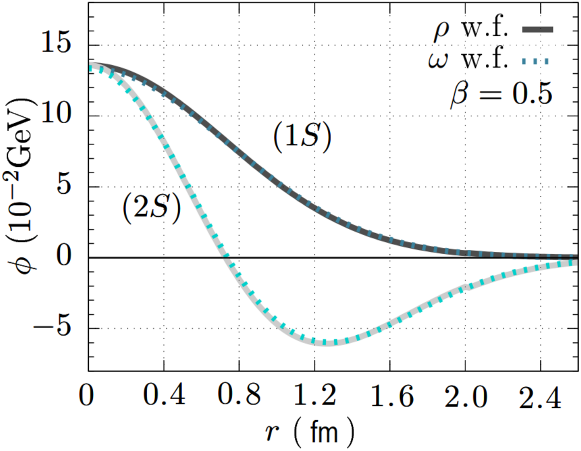

Dynamical part of the wavefunction of the ρ and ω mesons, as well as their excited states.

Differential Cross Section

We can now compute the differential cross section in t, as previously seen:

$$\mathcal{A}^{\gamma p}(x,t) = 2i \int d^2\mathrm{r} \int_0^1 d\beta \int d^2\mathrm{b} \Psi_V(r,\beta)\Psi_\gamma(r,\beta) \times e^{-i[\mathrm{b}-(1-2\beta)\mathrm{r}/2]\cdot\Delta} N(x,\mathrm{r},\mathrm{b})\,. \tag{10}$$

Thus:

$$\frac{d\sigma^{\gamma p\to Vp}}{dt}(W,t) = \frac{1}{16\pi}\left|\mathcal{A}^{\gamma p\to Vp}(W,t)\right|^2. \tag{11}$$

Considering the case of the integrated cross section, in the small t limit, we assume $\frac{d\sigma^{\gamma p \to Vp}}{dt} \propto \exp(-B_s t)$, with

$$\mathcal{A}^{\gamma p \to Vp}(W, t) \approx e^{-B|t|/2} \mathcal{A}^{\gamma p \to Vp}(W, t \approx 0) \,. \qquad (12)$$

where B_s is called the slope parameter (fitted to ZEUS data). We have,

$$B_s = N \left[14.0 \left(\frac{1 \mathrm{GeV}^2}{Q^2 + M_V^2} \right)^{0.2} + 1 \right] . \qquad (13)$$

Correction for the real part:

$$\mathcal{A}^{\gamma p} \to \mathcal{A}^{\gamma p} \left(1 - i \frac{\pi \lambda}{2} \right) \,, \quad \text{with} \quad \lambda = \frac{\partial \ln \mathcal{A}^{\gamma p}}{\partial \ln(1/x)} \,. \qquad (14)$$

and the *skewness effect*:

$$R_g(\lambda) = \frac{2^{2\lambda+3}}{\sqrt{\pi}} \frac{\Gamma(\lambda + 5/2)}{\Gamma(\lambda + 4)} \,. \qquad (15)$$

Integrated Cross Section for $\rho(1S)$

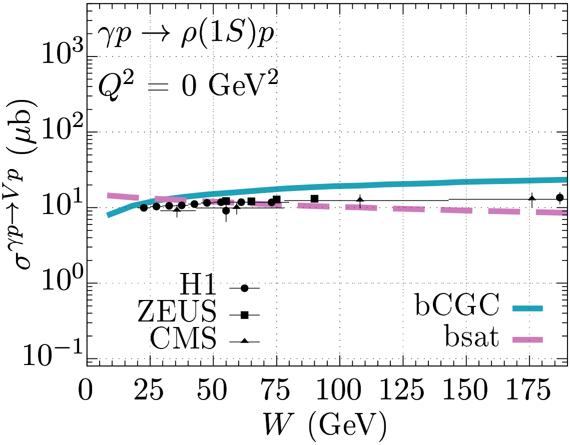

Total cross section for the photoproduction of $\rho(1S)$ as a function of the γp center-of-mass energy, W.

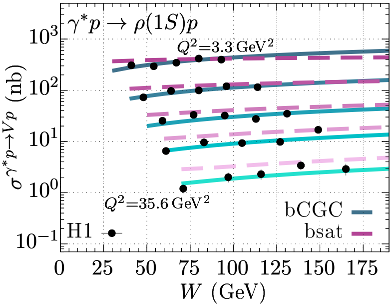

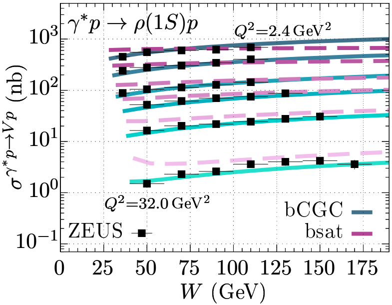

On the left, the obtained results are compared to H1 data. On the right, the results are compared to ZEUS data.

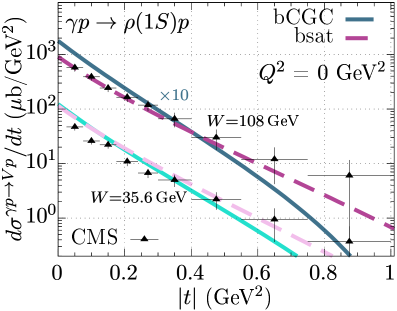

Differential cross section for the photoproduction of $\rho(1S)$ as a function of the squared momentum transfer t.

Differential Cross Section in t for Electroproduction of $\rho(1S)$

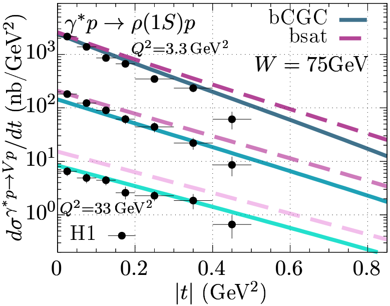

Differential cross section for the electroproduction of $\rho(1S)$ at $W = 75$ GeV.

Total and Differential Cross Section for $\omega(1S)$

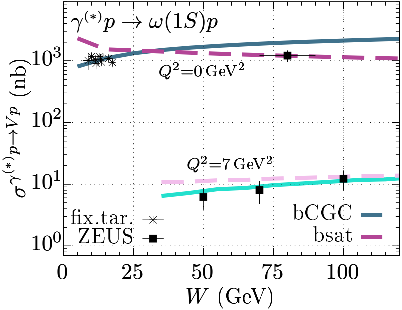

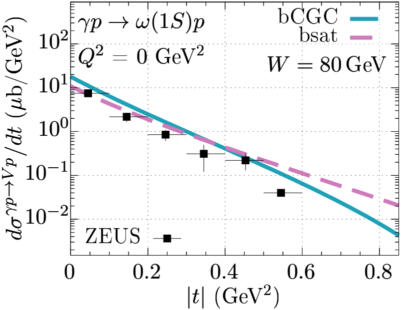

Results for the photo- and electroproduction cross sections of $\omega(1S)$. Fixed-target data is a compilation from several collaborations.

Total and Differential Cross Section for $\phi(1S)$

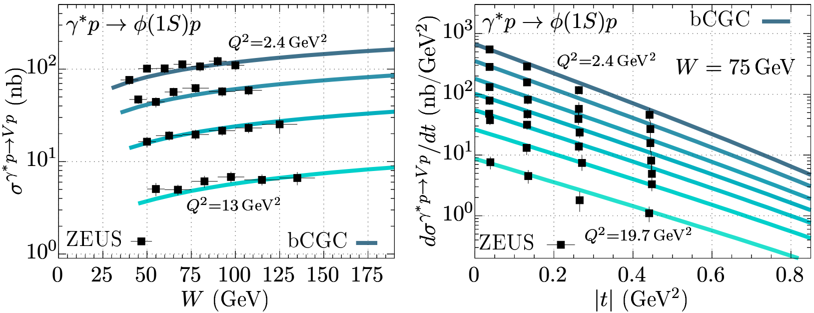

Numerical results for the electroproduction of $\phi(1S)$, compared with ZEUS data. On the left, from top to bottom. On the right, the differential cross section in t for $W = 75$ GeV.

Predictions for Excited States $\rho(2S)$, $\omega(2S)$, and $\phi(2S)$

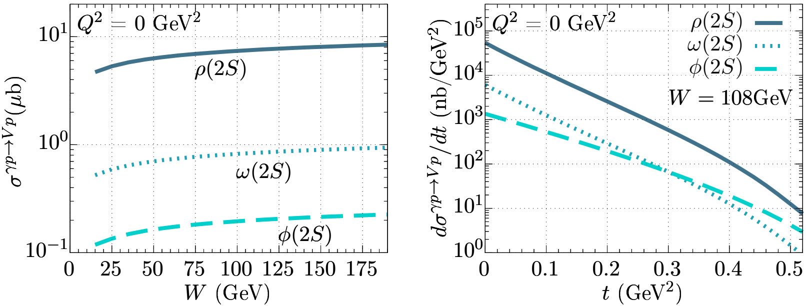

Predictions for the total photoproduction cross section as a function of W (left panel) and for the differential cross section in t (right panel) for $\rho(2S)$, $\omega(2S)$, and $\phi(2S)$.

Predictions for the Ratio Between Excited and Ground States

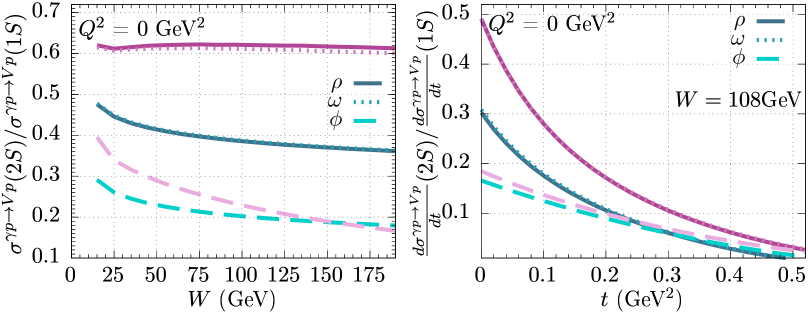

Predictions for the ratio of the total cross section between excited and ground states as a function of W (left panel) and for the ratio of the differential cross section in t, considering $W = 108$ GeV.

Photoproduction in Ultraperipheral Collisions of Two Lead Nuclei

Coherent and Incoherent Cross Sections

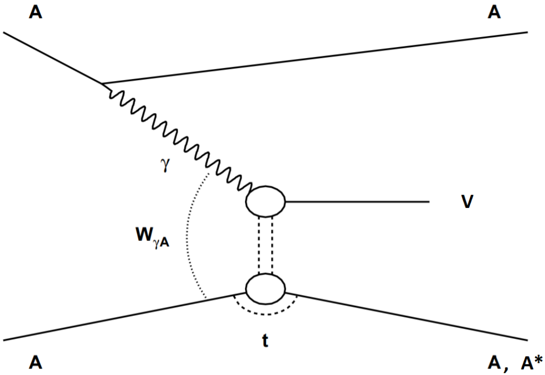

Nuclear photoproduction of a meson V in an ultraperipheral AA collision. The final state of the target nucleus A remains unchanged for the coherent case, while it changes to an arbitrary state A^* in the incoherent case.

Factorization

For photoproduction, we start with the factorization of the differential cross section:

$$\frac{d\sigma_{AA\to AVA}}{dy} = \omega \frac{dN_\gamma}{d\omega}\sigma_{\gamma A\to VA}(\omega)\,, \tag{16}$$

where

$$y = \ln\left(\frac{2\omega}{M_V}\right)\,, \quad x = \frac{M_V e^{-y}}{\sqrt{s_N}}\,. \tag{17}$$

Taking into account that either nucleus can act as the photon source, we must add a term to (16):

$$\frac{d\sigma_{\gamma A\to VX}}{dy} = \omega \frac{dN_\gamma}{d\omega}\sigma_{\gamma A\to VA}(\omega) + (y\to -y)\,. \tag{18}$$

Weizsäcker-Williams Flux Factor

Using the Weizsäcker-Williams method:

$$\frac{d^3N}{d\omega d^2\vec{b}_\gamma}(\omega,\vec{b}_\gamma) = \frac{1}{\pi^2}\frac{q^2}{b_\gamma^2}\left(\frac{\omega b_\gamma}{\gamma}\right)^2\left[\frac{1}{\gamma^2}K_0^2\left(\frac{\omega b_\gamma}{\gamma}\right) + K_1^2\left(\frac{\omega b_\gamma}{\gamma}\right)\right], \tag{19}$$

with $q = Ze$ and $v \approx c = \hbar = 1$. The photon flux is given by:

$$\omega\frac{dN_\gamma(\omega,b)}{d\omega} = \int d^2\mathrm{b}_\gamma \frac{\omega d^3N_\gamma(\omega,b_\gamma)}{d\omega d^2\mathrm{b}_\gamma} \exp\left(-\sigma_{\mathrm{NN}}^{\mathrm{tot}}\int d^2\mathrm{b}' T_A(b')T_A(|\mathrm{b}_{AA}-\mathrm{b}'|)\right) \tag{20}$$

The condition for an ultraperipheral collision is that the distance between the centers of the nuclei is greater than the sum of their radii, $2R_A$.

Coherent Cross Section

The coherent cross section can be obtained using:

$$\sigma_{el}^{hA\to hA} = \int d^2b \left|\langle 0|\Gamma_A^h(\vec{b})|0\rangle\right|^2 . \tag{21}$$

From Glauber theory, the amplitude $\Gamma_A^h(\vec{b})$ at high energies is written as:

$$\Gamma_A^h(\vec{b},\vec{s_i}) = \left\{1 - \prod_j^A [1 - \Gamma_N^h(\vec{b} - \vec{s_j})]\right\} \tag{22}$$

Therefore, the total coherent cross section becomes:

$$\sigma_{tot}^{hA} = 2\int d^2b \mathrm{Re}\left\{1 - \left[1 - \frac{1}{A}\int d^2s\Gamma_N^h(s)\int_{-\infty}^{\infty} dz\rho_A(\vec{b} - \vec{s}, z)\right]^A\right\}$$
$$\approx 2\int d^2b\left\{1 - \exp\left[-\frac{1}{2}\sigma_{tot}^{hN} T_A(b)\right]\right\} , \tag{23}$$

Gribov Correction

Considering only Glauber:

$$\sigma^{hA\to hA} = \int d^2b \left|1 - \exp\left[-\frac{1}{2}\sigma_{tot}^{hN} T_A(b)\right]\right|^2 . \qquad (24)$$

Gribov correction:

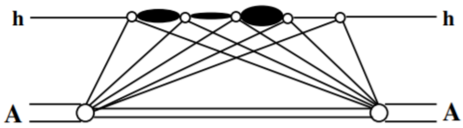

Diffractive excitations of the projectile hadron inside the nuclear medium to intermediate states. We must replace the meson-nucleon cross section with the dipole cross section:

$$\sigma^{\gamma A\to VA} = \int d^2b \left| \int d\beta d^2r \Psi_V^\dagger \Psi_\gamma \left[1 - \exp\left(-\frac{1}{2}\sigma_{q\bar{q}}(x,r) T_A(b)\right)\right] \right|^2 \qquad (25)$$

Nuclear Thickness Function

For the presented thickness function, we consider:

$$T_A(b) = \int_{-\infty}^{+\infty} dz\, \rho_A(b,z)\,, \qquad \frac{1}{A}\int d^2b\, T_A(b) = 1\,, \qquad (26)$$

where $\rho_A(b,z)$ is the nuclear density as a function of impact parameter b and longitudinal coordinate z. In this work, we use Woods-Saxon distributions:

$$\rho_A(b,z) = \frac{N_A}{1+\exp\left[\frac{r(b,z)-c}{\delta}\right]}\,, \qquad r(b,z) = \sqrt{b^2+z^2}\,, \qquad (27)$$

Here, r is the distance to the nucleus center, N_A is a normalization factor, and the parameters are $c = 6.62$ fm and $\delta = 0.546$ fm for lead (Pb).

Nuclear Photoproduction of ρ (GG)

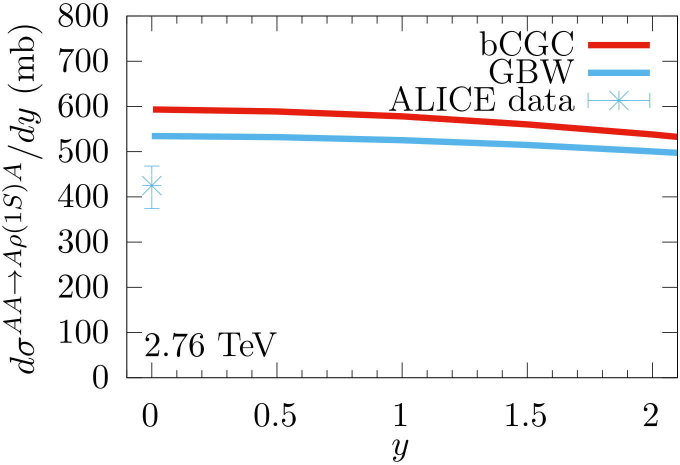

The results suggest the need for an effect that can suppress the cross section.

Gluon Shadowing in the Nuclear Medium

The nuclear phenomenon of gluon shadowing is expected, since the gluon density inside nuclei at high energies ($x \ll 1$) should be suppressed compared to a free nucleon due to interference effects.

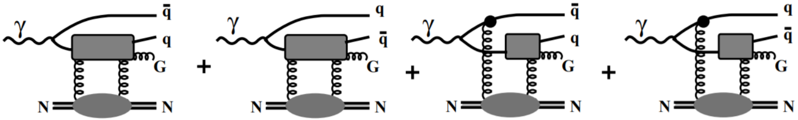

As we have no access to the dynamic variables, we reinterpret the phenomenon as a modification in the gluon density of the target ion.

Knowing that the dipole cross section is proportional to the gluon distribution g of the proton, we have:

$$\frac{\sigma^{A}_{q\bar{q}}}{\sigma_{q\bar{q}}} \approx \frac{xg_A(x,\mu^2)}{Axg_N(x,\mu^2)} \equiv R_g(x,\mu^2)\,. \tag{28}$$

Therefore, the dipole-proton cross section must be rescaled:

$$\sigma_{q\bar{q}} \Rightarrow \sigma_{q\bar{q}} R_G(x,\mu^2)\,. \tag{29}$$

In our previous works, using PDFs:

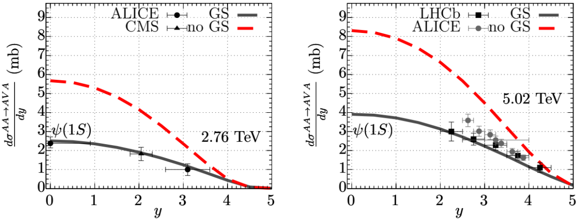

Nuclear Photoproduction Diagram

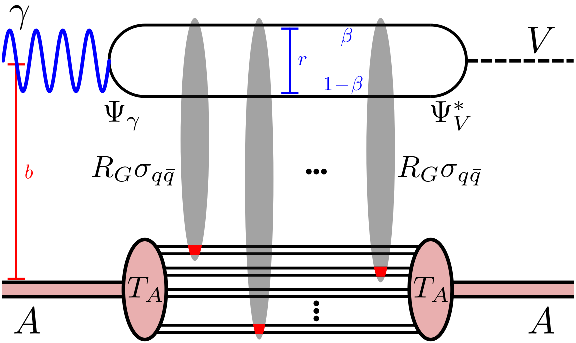

Diagrammatic illustration of the coherent photoproduction process of a vector meson (V) in $\gamma A \to VA$ scattering.

Issue: We do not have PDFs fitted at small scales, proportional to the masses of light vector mesons.

F_2^A Data at Small Q^2

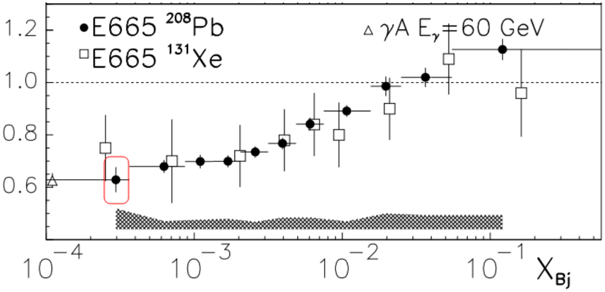

$F_2^A/(AF_2^p) = 0.628 \pm 0.048 \pm 0.079$, measured by the E665 collaboration (with $x_{\rm Bj} \subset (1-3.7)\cdot 10^{-4}$ and $\langle Q^2 \rangle = 0.15$ GeV^2).

Effective R_G: Fitted to the F_2^A data point and experimental data from coherent production $PbPb \to \rho(1S)PbPb$.

Effective R_G

For the nuclear structure function F_2^A, we have:

$$F_2^A = F_L^A + F_T^A = \frac{Q^2}{4\pi^2\alpha_{em}} \left(\sigma_T^{\gamma^* A} + \sigma_L^{\gamma^* A}\right) , \tag{30}$$

where the transverse and longitudinal total cross sections are:

$$\sigma_{T,L}^{\gamma^* A} = \sum_q \int d^2 r \int_0^1 d\beta |\Psi_{T,L}(r, \beta, m_q)|^2 \sigma_{q\bar{q}}^A(r, x) . \tag{31}$$

Here, $\sigma_{q\bar{q}}^A(r, x)$ is obtained via Glauber–Gribov, similarly to earlier:

$$\sigma_{q\bar{q}}^A(r, x) = 2 \int d^2 b \left[1 - \exp\left(-\frac{1}{2} A T_A(b) \sigma_{q\bar{q}}(r, x)\right)\right] . \tag{32}$$

Description of $PbPb \to \rho(1S)PbPb$

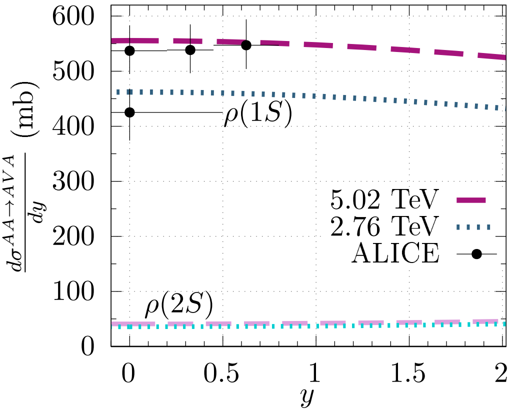

Differential rapidity cross section for the coherent photoproduction of $\rho(1S, 2S)$, calculated using the GBW dipole model. The gluon shadowing effect is fitted: $R_G = 0.85$.

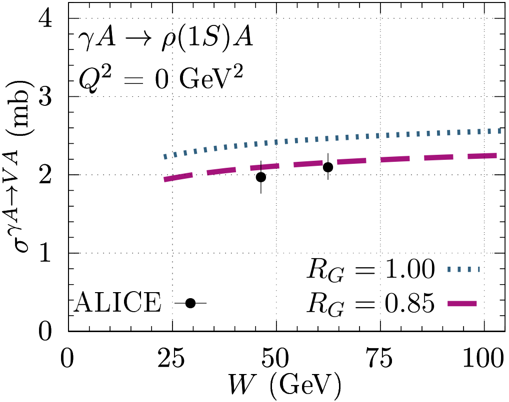

Photoproduction of $\rho(1S)$ in the γPb subprocess as a function of the center-of-mass energy W, calculated using the GBW dipole model.

Photoproduction of $\omega(1S, 2S)$

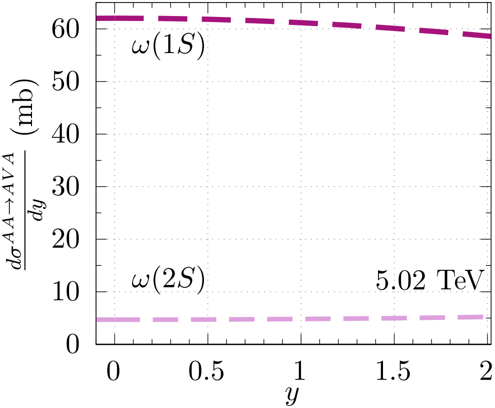

Predictions for the differential cross section in y for coherent photoproduction of $\omega(1S, 2S)$ in ultraperipheral PbPb collisions, calculated using the GBW dipole model.

Photoproduction of $\phi(1S, 2S)$

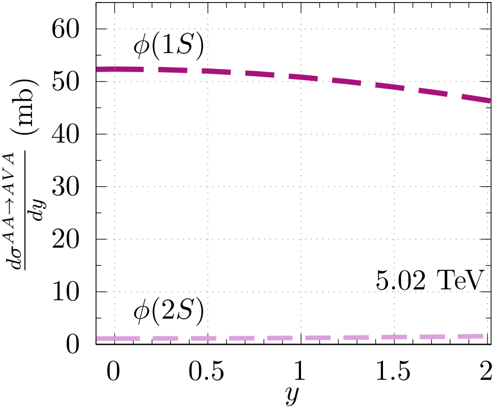

Predictions for the differential cross section in y for coherent photoproduction of $\phi(1S, 2S)$ in ultraperipheral PbPb collisions, calculated using the GBW dipole model.

Cross Section Ratio

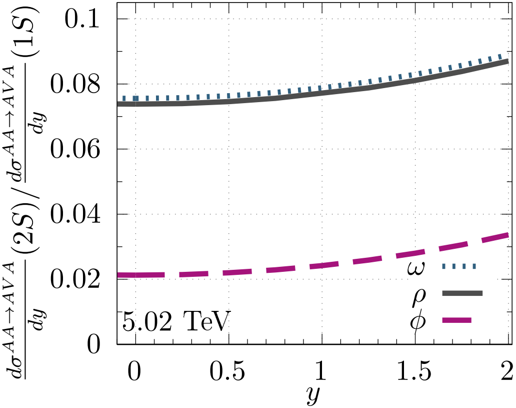

Predictions for the ratio of the photoproduction cross section of excited states to ground states, calculated using the GBW dipole model.

Additional Results for $\phi(1S)$ at LHCb and CMS

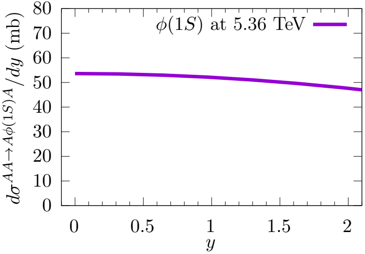

Coherent photoproduction of $\phi(1S)$ for CMS Run 3 (central rapidity).

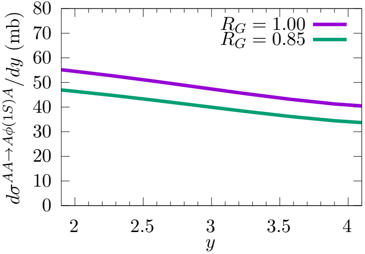

Coherent photoproduction of $\phi(1S)$ for LHCb (forward rapidity).

In April this year, CMS obtained data for $\phi(1S)$!

Comparison with CMS Data

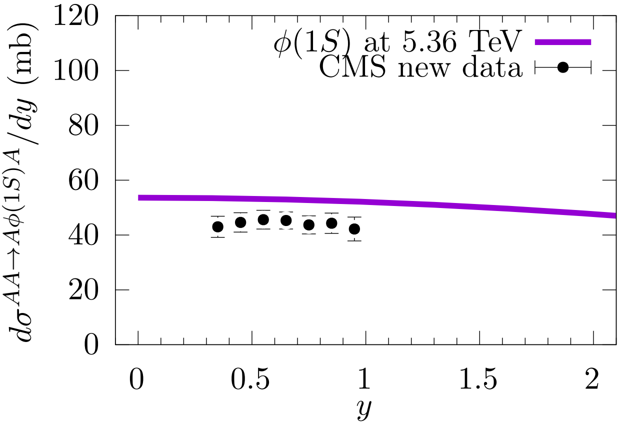

The GBW model and $R_G = 0.85$ were used. The coherent photoproduction data for $\phi(1S)$ suggest the need for an even stronger shadowing effect, which was already anticipated.

Conclusions

- We studied exclusive photoproduction and electroproduction of light vector mesons (ρ, ω, and ϕ) within the color dipole formalism.
- We used bCGC and bSat dipole models, achieving good agreement with electroproduction data ($Q^2 > 0$).
- Meson wavefunctions were modeled using the holographic QCD approach in light-cone formalism, solving a Schrödinger-like equation with an effective confinement potential.
- The importance of a meson-mass-dependent effective confinement parameter κ was identified.
- A common formalism allows evaluation of different contributions and theoretical uncertainties in the calculations.

Conclusions

- Sensitivity to the choice of color dipole parametrization was observed.
- The holographic approach enables predictions for excited states like $\rho(2S)$, $\omega(2S)$, and $\phi(2S)$—a rarity in the literature.
- We extended the formalism to nuclear photoproduction (Glauber–Gribov), motivated by new LHC data for $AA \to \rho(1S)AA$.
- The $Pb\,Pb \to \rho(1S)\,Pb\,Pb$ data indicate the need to include a nuclear suppression effect.
- This effect can be interpreted as gluon shadowing, adjusted to an effective value of $R_G = 0.85$.
- Predictions for $\rho(1S, 2S)$, $\omega(1S, 2S)$, and $\phi(1S, 2S)$ are presented.

Acknowledgements

Thank you!